Design and Development of RED-Data2: A Data Recording Reentry Vehicle

AE8900 MS Special Problems Report
Space Systems Design Lab (SSDL)
Guggenheim School of Aerospace Engineering
Georgia Institute of Technology
Atlanta, GA

Author:
Adam T. Sidor

Advisor:
Dr. Robert D. Braun

August 1, 2014

Design and Development of RED-Data2: A Data Recording Reentry Vehicle

Adam T. Sidor * and Robert D. Braun †

Georgia Institute of Technology, Atlanta, GA, 30332

Defunct, manmade objects in orbit regularly reenter Earth's atmosphere in an uncontrolled manner causing risk of both personal injury and property damage. To reduce uncertainty and improve our ability to predict surviving debris, impact time and impact location, reentry breakup dynamics and aerothermodynamics data is needed. The Reentry Breakup Recorder has demonstrated the ability to obtain inertial and thermal measurements during reentry that are pertinent to spacecraft breakup. Building on this concept, the present investigation explores the design space for this device and matures a smaller, lighter and more operationally flexible system, termed RED-Data2.

Nomenclature

β	Ballistic coefficient
$C_D A$	Drag area
r	Planet-centric radius
V	Planet-relative velocity
V_0	Planet-relative velocity at entry interface
γ	Flight path angle
γ_0	Flight path angle at entry interface
ψ	Heading angle
ψ_0	Heading angle at entry interface
λ	Latitude
θ	Longitude
ϕ	Zenith angle
ρ	Atmospheric density
ω	Planet rotational rate
$\dot{q}_s$	Instantaneous stagnation heat rate
J_s	Integrated stagnation heat load
D	Maximum capsule diameter
R_n	Capsule nose radius
RED	Reentry Device
TPS	Thermal Protection System
IMU	Inertial measurement unit
RTC	Real time clock
AFC	Avionics Flight Computer
EBM	Expansion Board Module

I. Introduction

SPACE debris, a collection of defunct satellites, spent rocket stages, and other manmade objects, routinely reenter Earth's atmosphere. Most objects below a certain size and mass break up and disintegrate in

*Graduate Research Assistant, Guggenheim School of Aerospace Engineering.

†David and Andrew Lewis Professor of Space Technology, Guggenheim School of Aerospace Engineering

the high heating and loading environment of reentry before ever reaching the ground. However, large, massive objects can and do regularly survive reentry, posing a risk to people and property. The incidence of such events will increase as more objects are placed into orbit and on-orbit collisions expand the orbital debris population. If possible, operators strive to deorbit an object in the ocean away from populated areas. However, even in these controlled entries, large uncertainties often exist in the footprint of the resulting debris. Furthermore, controlled deorbit often has associated negative economic or mission operations penalties.

Current reentry survivability models tend to under-predict the occurrence of space debris surviving to the ground. To better quantify the reentry environment and, ultimately, improve reentry safety, analysts must validate and improve models. Relevant environment flight data collected onboard a reentering spacecraft is key to this work. The Aerospace Corporation initially conceived of a device to address such a need in the early 2000s – the Reentry Breakup Recorder (REBR).[1–3] REBR was flown in 2011 and 2012 as an attached payload on four resupply missions to the International Space Station (ISS).

RED-Data2 is a next-generation reentry breakup recorder that leverages the REBR design, under license from The Aerospace Corporation. It improves upon the size, mass and functionality over the past design while providing greater operational flexibility. The vehicle itself is 20cm at maximum diameter (approximately equal to the diameter of a regulation soccer ball) and 1.43 kg (3.15 lbs). Redesigned electronics and flight software allow it to function autonomously for a range of potential missions, expanding on REBR which flew to and from the ISS only and required manual activation. Thus, RED-Data2 is easily integrable as a standalone, secondary payload on a host spacecraft. The range of flight data returned includes 3-axis accelerations and rotational rates, temperatures and pressure during the reentry and breakup event. This paper documents the development of RED-Data2 from concept to final design.

II. Historical Perspective

In recent years, much attention, both inside and outside the space community, has been garnered by the rise of miniaturized satellites. Dubbed smallsats, these spacecraft encompass a broad range of functionalities – from remote sensing to communications to reconnaissance – in packages below 500kg. Nanosatellites, a subcategory of smallsat with masses in the 1-10kg range, have experienced explosive growth due in large part to the CubeSat protocol first introduced in 1999. Nanosatellites have attracted increasing research and development activities in the last decade. From 2000-2005, nanosatellite launches averaged 5.2 per year. From 2006-2011, this number increased to 15.5 per year on average. In the past two full years, the number of launches has continued to accelerate with 26 and 85 launches in 2012 and 2013, respectively.[4]

Smallsats are revolutionizing our ability to get into space. Reaching Earth orbit is now more frequent and more accessible than ever. In contrast, returning to Earth, ignoring uncontrolled entries of space debris and controlled entries intended only to destroy the spacecraft, is significantly less common. Historically, Entry, Descent and Landing (EDL) has been the domain of large budget and/or large scale endeavors – e.g., manned vehicles such as the Space Shuttle and Soyuz capsule and unmanned vehicles such as Space Exploration Technologies' Dragon and NASA's Stardust Sample Return Capsule (SRC). Miniaturized reentry probes, somewhat analogous to smallsats, have been posited as a cost effective and accessible means for returning from space.[5,6] These probes can facilitate a range of scientific and engineering functions including data collection, flight testing and payload return. Recent interest in small reentry probes include the aforementioned REBR, the Japanese-developed iBall reentry recorder, and a family of other small ReEntry Devices (REDs) under joint development with Terminal Velocity Aerospace, LLC.[7]

II.A. Design Heritage

Small reentry probes have an extensive heritage within EDL having been employed in a variety of entries both at Earth and other planetary bodies. As direct predecessors to RED-Data2, Mars Microprobe and REBR are the most influential to the design. Other small entry vehicles include the Stardust and Hayabusa sample return capsules and i-Ball reentry recorder.

II.A.1. Mars Microprobe

Mars Microprobe is a 3.6kg, 0.35m diameter capsule. The forebody is a 45° half-angle conical segment with spherical nose – a so-called 45° sphere-cone. The nose radius, R_n, is $0.25D$ while shoulder radius is $0.025D$. The aftbody is a $0.52D$ radius hemisphere. Two identical Microprobes were flown in 1999 as secondary

payloads aboard Mars Polar Lander.[8] Mars Microprobe was designed to enter the Martian atmosphere and impact the Martian surface at high velocity. Its high impact velocity allowed it to penetrate the surface to a depth of about 10cm to return data on soil composition and properties.

To successfully penetrate the surface, Microprobe had to maintain a small attitude tolerance for the entire trajectory up to and including impact. However, mission constraints did not allow active guidance. Achieving the required attitude tolerance within this constraint necessitated the unique outer mold line geometry of Figure 1. The resulting design possesses a superior ability to reorient during hypersonic flight and maintains stability through the transonic and subsonic regimes without active control mechanisms or supplemental drag devices.[9,10]

II.A.2. Reentry Breakup Recorder

REBR employed the Mars Microprobe 45° sphere-cone geometry in an approximately 4kg, 0.31m diameter capsule. The REBR concept was first introduced in 2003.[3] The concept of operations for a reentry recorder (discussed in the next section) was initially proposed in this work. REBR carries an electronics package that includes a flight computer board and sensor board. Its onboard sensors include accelerometers, gyroscopic sensors and thermocouples for recording acceleration, attitude and temperature of the host spacecraft. It is powered by two sets of 24 AA cells which, along with the electronics, are assembled to an aluminum and plastic chassis and installed into the aeroshell. The vehicle is enclosed in a two-piece copper housing which mounts to the host spacecraft via a skirt and adapter ring. An assembly view and flight unit are shown in Figure 2.

REBR flew four times aboard ISS resupply missions – two aboard the H-II Transfer Vehicle (HTV-2, -3) and two aboard the Automated Transfer Vehicle (ATV-2, -3). Three of these successfully returned data (the unit aboard ATV-2 did not return data and was suspected to have not survived breakup). The REBR design was subsequently licensed from Aerospace Corporation for RED-Data2 development.

II.A.3. Other Small Entry Vehicles

Sample return missions Stardust and Hayabusa both utilized small entry capsules to return samples from Solar System bodies. Stardust was a NASA Discovery-class mission to rendezvous with Comet Wild-2, collect samples and return them safely to the Earth. Launched in 1999, Stardust encountered the comet in 2004 and returned to earth in 2006. The Stardust SRC protected the samples during Earth entry and recovery. The SRC is a 0.8128m diameter, 45.6kg capsule. The forebody is a 60° sphere-cone with $R_n = 0.28125D$. A 30° half-angle conical section forms the aftbody.[11] Its combination of high entry velocity (12.9 km/s) and small size produced a stagnation point heat rate of 1100 W/cm^2, the highest of any Earth entry at the time.

Hayabusa, developed by the Japan Aerospace Exploration Agency (JAXA), launched in 2003 and visited asteroid Itokawa in 2005. The Hayabusa SRC is a 16.3kg, 0.4m diameter 45° sphere-cone with conical aftbody.[13] It is configured with a $0.5D$ radius nose. After several technical setbacks which delayed return, its SRC reentered Earth's atmosphere in 2010. Both entry capsules are depicted in Figure 3.

i-Ball is a reentry recorder that includes two video cameras to record reentry and breakup. A 15.5kg, 40cm diameter spherical capsule, i-Ball is a joint development of JAXA and IHI Aerospace Co.[a]

III. Concept of Operations

The concept of operations for RED-Data2 is outlined in Figure 4 for an uncontrolled, orbital decay entry. A nearly identical concept of operations is followed in a controlled entry, except a deorbit burn initiates reentry. The mission can be separated into four phases: Pre-Launch and Launch, Reentry Detection, Data Recording and Data Transmission.

III.A. Pre-Launch and Launch

Initially, the device is activated on the ground before final assembly and installation into its host spacecraft. Upon activation, the electronics will perform a brief check to assure the hardware is functioning properly. When the system check passes, the hardware will enter into a low power sleep mode with most of the electronics powered off. Then, the assembled vehicle is installed inside the host to await launch.

[a] http://www.spaceflight101.com/htv-3-cargo-manifest.html

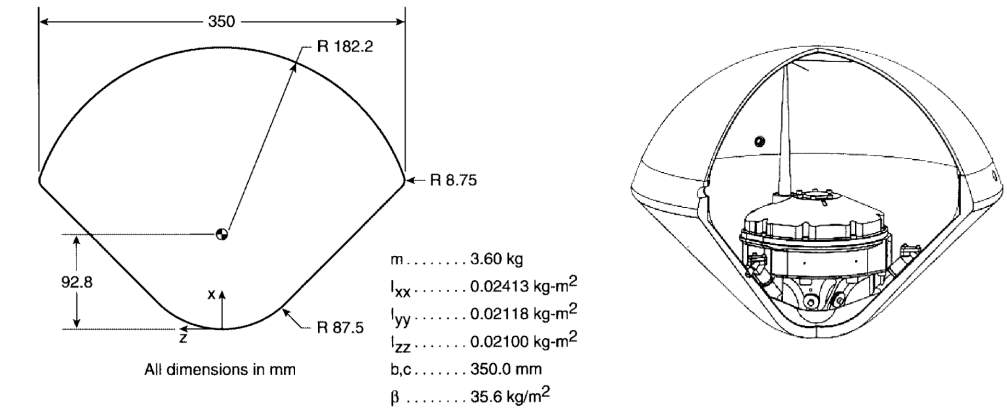

Figure 1: Mars Microprobe outer mold line and mass properties[10] (left) and cutaway view[8] (right).

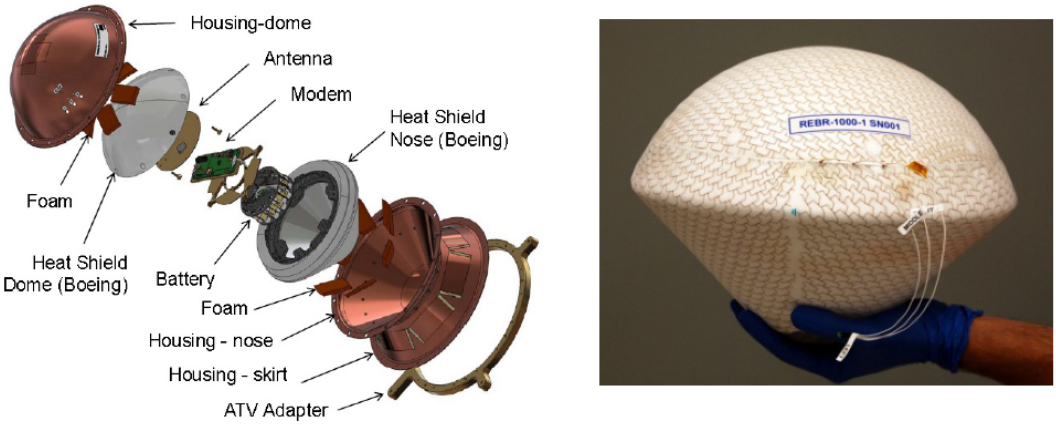

Figure 2: REBR exploded view (left) and flight unit (right).[1]

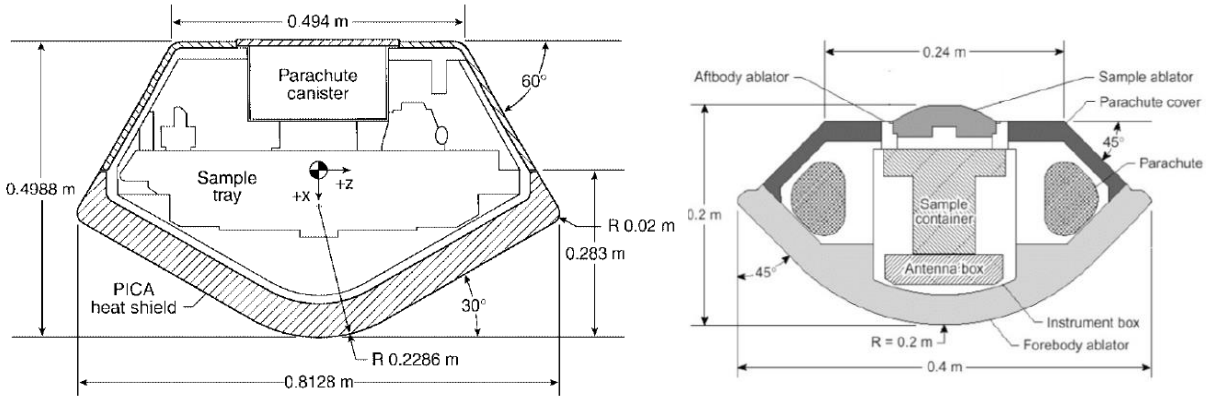

Figure 3: Stardust[12] and Hayabusa[13] entry capsule configurations (not to scale).

III.B. Reentry Detection

After launch, the device wakes from sleep and enters a reentry detection mode. In this phase, a subset of the electronics hardware, the reentry detection circuit, is powered on while the rest remains off. Reentry detection remains active for the entirety of the host's on-orbit operations (up to a year or more). This requires the detection algorithm to reject non-reentry acceleration events, which is described in more detail later. At the conclusion of on-orbit operation, a deorbit burn is performed to deorbit the host, or, in an uncontrolled entry, orbital decay due to exoatmospheric drag will cause reentry. In either case, reentry detection, triggered by increasing drag during atmospheric flight, activates the remaining hardware.

III.C. Data Recording

With the electronics fully active, the vehicle now reads and stores data from a suite of sensors. Depending on the steepness of the entry, recording occurs for anywhere from 1–4 minutes. Eventually, the host breaks apart and RED-Data2 is released. Here, data recording can either continue, if interested in obtaining data at other points in the trajectory (e.g., peak heating and/or peak deceleration), or terminate, if only interested in the host dynamics.

III.D. Data Transmission

When data recording terminates, the device begins to attempt communiction with the Iridium satellite network. When connection is established, the recorded data is transmitted through Iridium to a ground server. Data uplink must occur before impact as the vehicle is not designed for recovery.

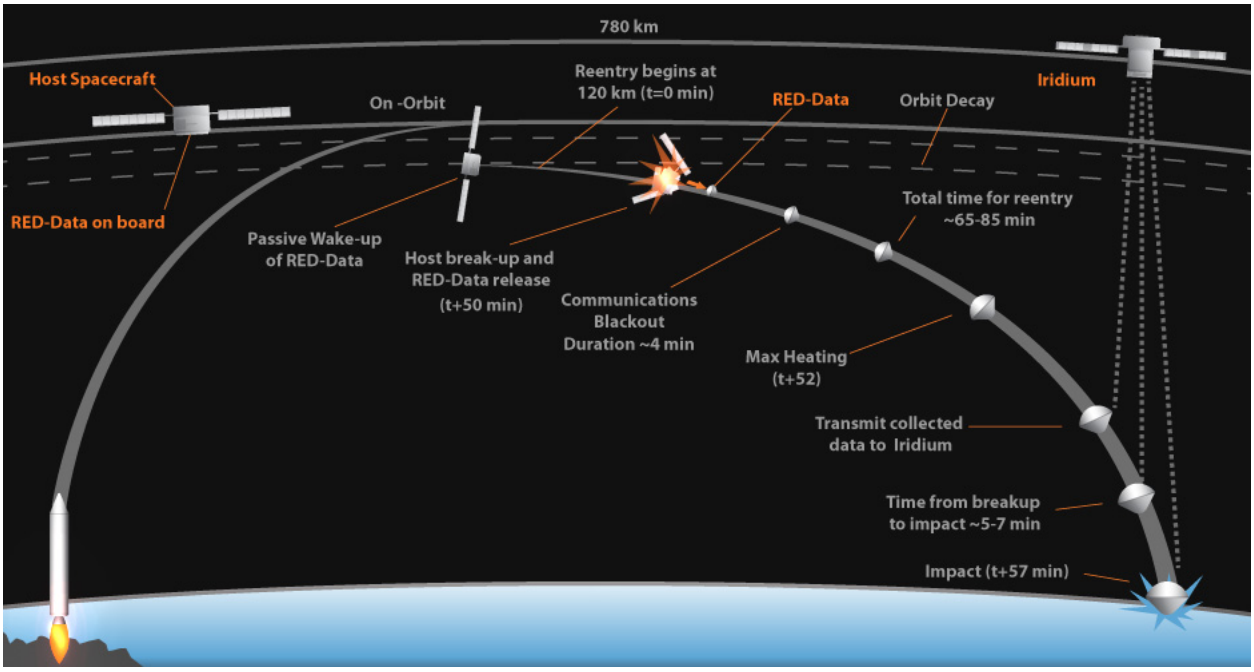

Figure 4: Concept of Operations for RED-Data2.

IV. Objectives

REBR demonstrated the potential for reentry data return by a small probe. As a proof-of-concept only, however, its usage is limited to all but a small subset of host spacecraft. Manual activation in space before reentry effectively limits it to ISS missions. Additionally, its lifetime, after activation, is a maximum of one month, which does not accommodate longer term orbital missions.

While RED-Data2 is similar to REBR in both form and function, it is a largely new design. Key components and design features have been retained for RED-Data2 where it is advantageous (e.g., batteries and a subset of sensors). However, the present design is constructed from the "ground up" in order to increase

its utility as a data recorder and minimize its impact on the host spacecraft. It is intended as a lightweight, low cost, flexible secondary payload that is accessible to a broad range of satellite and spacecraft providers. To achieve this end, several objectives, outlined in Table 1, guide the design of RED-Data2. Objectives are categorized as issues of utility, host impact, and/or accessibility.

Table 1: RED-Data2 Design Objectives.

Objective	Category	Reason
Minimize size and mass	Host impact	Easy accommodation in host design
Limit unit cost	Host impact / Accessibility	Minimal impact on host budget; cost feasibility for providers
Limit manufacturing complexity	Accessibility	Rapid, low cost production
Match or exceed total data return of REBR	Utility	Maintain or improve device usefulness
Operate autonomously for entire mission	Utility	No manual activation required; accommodate non-ISS missions
Return data for arbitrary LEO entries	Utility	Accommodate larger range of missions
Increase lifetime	Utility	Accommodate larger range of missions

V. Methodology

The conceptual and final designs described in this paper were evaluated by simulating trajectories from entry interface to host breakup and from host breakup to the ground. Stagnation point heat rate, integrated heat load and peak deceleration were estimated from resulting trajectories.

V.A. Simulated Trajectory

V.A.1. Equations of Motion

Three-degree-of-freedom, ballistic (non-lifting) trajectories are simulated via equations of motion, adapted from Ref. 14, formulated in a planet-centric, planet-fixed frame. A spherical, rotating planet with atmosphere at rest relative to the planet is assumed. The governing equations are shown in Eqs. (1) – (6), where r is planet-centric position, V is planet-relative velocity, γ is flight path angle, ψ is heading angle, and λ and θ are latitude and longitude, respectively. Flight path angle is measured relative to the local horizontal and is defined as positive above the horizon. Heading equals 0° when traveling eastward and is positive in the right-handed direction. D denotes the drag force, $\frac{1}{2}\rho V^2 C_D A$. Atmospheric properties are obtained from the 1976 U.S. Standard Atmosphere, and gravity follows an inverse-square model.

$$\dot{r} = V \sin\gamma \tag{1}$$

$$\dot{V} = \frac{-D}{m} + \omega^2 r \cos\lambda \left(\sin\gamma\cos\lambda - \cos\gamma\sin\lambda\sin\psi\right) - g\sin\gamma \tag{2}$$

$$\dot{\gamma} = \frac{V\cos\gamma}{r} + 2\omega cos\lambda\cos\psi + \frac{\omega^2 r}{V}\cos\lambda\left(\cos\gamma\cos\lambda + \sin\gamma\sin\lambda\sin\psi\right) - \frac{g\cos\gamma}{V} \tag{3}$$

$$\dot{\psi} = -\frac{V}{r}\cos\gamma\cos\psi\tan\lambda + 2\omega\left(\tan\gamma\cos\lambda\sin\psi - \sin\phi\right) - \frac{\omega^2 r}{V\cos\gamma}\sin\lambda\cos\lambda\cos\psi \tag{4}$$

$$\dot{\lambda} = \frac{V\cos\gamma\sin\psi}{r} \tag{5}$$

$$\dot{\theta} = \frac{V\cos\gamma\cos\psi}{r\cos\lambda} \tag{6}$$

The entry occurs in two distinct phases, before and after breakup. Before breakup, RED-Data2 is internally attached to the host spacecraft, and the trajectory is that of the combined system. After breakup, RED-Data2 is separated and flies freely. The transition between the two occurs instantaneously at a given

breakup altitude that is specified a priori. Based on REBR analysis and flight data, this altitude is assumed between 65km and 85km.[1]

The transition is modeled as a change in the mass, m, and drag area, $C_D A$, that is a change in the ballistic coefficient,

$$\beta = \frac{m}{C_D A} \tag{7}$$

Before breakup, the ballistic coefficient is held constant. Thus, changes to the mass and drag area of the host during the breakup process are not captured. After breakup, the entry capsule is modeled with constant mass and Mach-dependent drag area.

V.A.2. Initial Conditions

The initial entry state is defined by the altitude, velocity, flight path angle, heading angle, latitude and longitude at entry interface. Two nominal cases are considered, (1) an orbital decay trajectory characterized by a very shallow entry flight path angle and entry velocity near the circular velocity and (2) an ISS return trajectory similar to the HTV and ATV entries flown with REBR onboard. The host is based on the ATV, the heavier of the two resupply vehicles, in the ISS return and on the Gravity Field and Steady-State Ocean Circulation Explorer (GOCE), which recently reentered in an uncontrolled deorbit, for the orbital decay entry. Entry is assumed to occur at 0° latitude resulting in an initial heading angle equivalent to the nominal orbital inclination. Entry parameters for both cases are outlined in Table 2.

Table 2: Parameters at Entry Interface.

Case	Altitude (km)	V_0 (km/s)	γ_0 (deg)	ψ_0 (deg)	Host β (kg/m^3)
Orbital Decay	125	7.74	-0.1	96.7	396
ISS Return	125	7.57	-1.4	56.1	444

V.A.3. Transmit Time

Transmit time is the period between first visibility to the Iridium network and ground impact. During this span, collected data can be transmitted from the reentry capsule. A zenith angle criteria based on REBR analyses, $\phi \leq 10°$, was adopted to quantify Iridium visibility where zenith angle, $\phi = \gamma + 90°$.[1] That is, at $\phi = 10°$ ($\gamma = -80°$), data transmission begins.

V.B. Aerothermodynamic Heating

RED-Data2 is assumed to encounter no heating prior to breakup while it is contained within the host spacecraft. At breakup, RED-Data2 becomes instantaneously exposed to aerothermodynamic heating.

Stagnation point heat rate was estimated via the Sutton-Graves relation for convective heating reproduced in Eq. (8).[15] Here, ρ is the local atmospheric density and R_n is the capsule nose radius. The constant k is atmosphere-dependent (at Earth, $k = 1.7415 \times 10^{-4}$).

$$\dot{q}_\mathrm{s} = k \left(\frac{\rho}{R_n} \right)^{1/2} V^3 \tag{8}$$

Radiative heating is neglected because it is assumed to be small relative to convective heating due to low entry velocity and small capsule size, an assumption which was later validated by more sophisticated analysis. Integrated heat load at the stagnation point, J_s, is computed by numerically integrating $\dot{q}_s$ from breakup to the ground.

$$J_\mathrm{s} = \int_{t_\mathrm{breakup}}^{t_\mathrm{ground}} \dot{q}_s \mathrm{d}t \tag{9}$$

Again, heating before breakup is assumed to be negligible.

VI. Concept Selection

VI.A. Procedure

A concept study was undertaken to select the baseline RED-Data2 design. While appealing because of its REBR and Mars Microprobe heritage, the 45° sphere-cone was not an immediate choice for RED-Data2. Thus, several aeroshell geometries and methods of payload packaging were compared. Three geometries were considered: a slender (12.5°) sphere-cone, a 45° sphere-cone and a sphere. With regard to thermal protection system (TPS) sizing, two different bondline temperature limits were considered for each concept, 125°C and 250°C. The trade space is outlined in Table 3.

Table 3: Concept study trade space.

Aeroshell Geometry	Bondline Temperature
12.5° Sphere-Cone	125°C
45° Sphere-Cone	250°C
Sphere	

Recognizing the need to reduce the overall size of the vehicle, the design methodology followed an inside-out approach (Figure 5). That is, the vehicle was designed around the payload (the electronics and instrument package) to maximize packing efficiency and create as small of a device as possible. The largest internal components (the Iridium modem and batteries) drive the overall size. Each concept design started with a layout and orientation for the payload components, then a basic aluminum structure was sized around it. Finally, the TPS thickness was sized to the target bondline temperature.

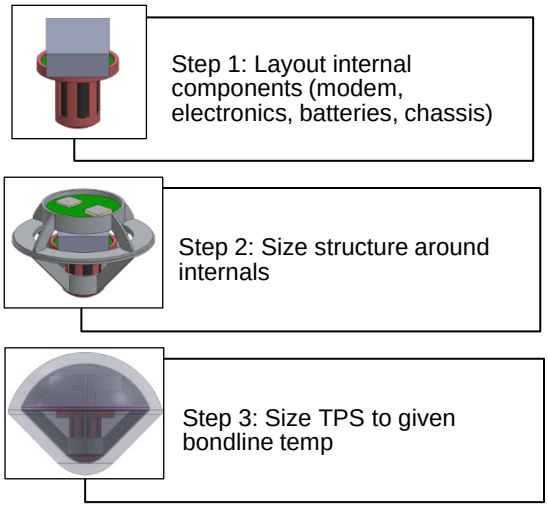

Figure 5: Inside-out design approach.

For each concept generated, several figures of merit were produced for comparison. These included (1) size metrics: estimated mass and maximum diameter, and (2) performance metrics: in-space lifetime, transmit time, peak deceleration, peak heating and integrated heat load. The intent of the size metrics is obvious; however, the performance metrics warrant further explanation. Peak heating is the maximum aerothermodynamic heat rate encountered by the vehicle during entry and drives TPS material selection and size. Data transmit time is a surrogate for total data return. The data return of RED-Data2 is dependent on the time and bandwidth of the Iridium call placed during descent as well as sensor sampling rates and precision. With a given transmit time and known transmission rate, the total data return in bytes can be backed out and used to inform sampling.

VI.B. Results

The spherical concept was quickly eliminated due to mass and performance concerns. This geometry exhibited larger mass in comparison to the other concepts which drove its ballistic coefficient higher and negatively impacted performance. The 45° sphere-cone and slender sphere-cone concepts were deemed the most competitive. Results for all concepts are shown in Table 4. Data is for an ISS return with breakup altitude of 75km. Note that TPS sizing is not available for REBR. Mass, maximum diameter and ballistic coefficient for REBR are actual values from the HTV-2 mission.[1] All other figures of merit were estimated in this study. It bears mentioning that the REBR flown on ATV-2 was slightly lighter at 3.95kg.

Due to ballistic coefficient considerations, the peak heating and transmit time of the 45° sphere-cone significantly outperforms the slender sphere-cone. The total transmit time is effectively doubled while peak heating is 56% less. Additional considerations also pointed to a 45° sphere-cone design – particularly its superior aerodynamic stability note previously. Also, the shape is an efficient one – it was estimated that mass and size growth would be limited if the payload grows in the future. Based largely on these considerations,

Table 4: Selected figures of merit, RED-Data2 concepts and REBR.

	REBR	Sphere	45° Sphere-Cone	12.5° Sphere-Cone
Mass (kg)	4.44	2.36	1.92	1.82
TPS Thickness (cm)	–	1.55	1.55	1.98
Bondline Temperature (°C)	127	250	250	250
Maximum Diameter (cm)	31.0	19.0	21.2	18.5
Hypersonic Ballistic Coefficient (kg/m^2)	55.4	83.4	51.2	174.6
Transmit Time (s)	359.8 (est.)	190.3	377.4	187.5
Peak Heating (W/cm^2)	203.3 (est.)	219.2	239.9	374.4

the 45° sphere-cone was selected as the baseline geometry for RED-Data2.

VII. Design

VII.A. Overview

The final RED-Data2 design is a small, lightweight, low cost and operationally flexible vehicle that compares favorably to the REBR design (Table 5). In addition to decreases in size and mass, RED-Data2 expands the capabilities of a reentry recorder enabling longer total mission lifetime (greater than one year) and autonomous, unmonitored operation. Advances in materials (particularly TPS materials) reduce manufacturing complexity and unit cost. The improved design can ultimately ease the adoption of reentry recorders by spacecraft providers increasing the accessibility to, and availability of, reentry data for breakup modeling and risk assessment.

Table 5: Comparison of final RED-Data2 and REBR Designs.

	ReBR	RED-Data2	% Improvement
Mass (kg)	4.44	1.43	68%
Maximum Diameter (cm)	31.0	20.0	35%
Hypersonic Ballistic Coefficient (kg/m^2)	55.4	42.9	23%
Transmit Time (s)	360	418	16%
Total Mission Lifetime (years)	0.1	>1	>1000%

VII.B. Vehicle

RED-Data2 is nominally a 1.43kg, 20 cm diameter 45° sphere-cone based on the Mars Microprobe geometry. The outer mold line is shown in Figure 6a. It consists of two primary systems: the aeroshell and payload, which further divided into several subcomponents (Figure 6b). Vehicle mass includes a component-specific contingency based on relative technology readiness and an overall 10% margin. A breakdown is provided in Table 6. Note that the TPS sizing already includes margin and, thus, no contingency is added for the forebody and aftbody TPS. The aeroshell (TPS, structural shells and assembly ring) comprises the majority of the total mass (0.705kg including contingency, or 54% of total mass). Payload mass, including contingency, totals 0.595kg (46% of total mass).

VII.B.1. Aerodynamics

RED-Data2 has a nominal hypersonic ballistic coefficient of 42.9 kg/m^2, based on a hypersonic drag coefficient, $C_D = 1.062$, and reference area of 0.031 m^2. Aerodynamic properties of the 45° sphere-cone geometry

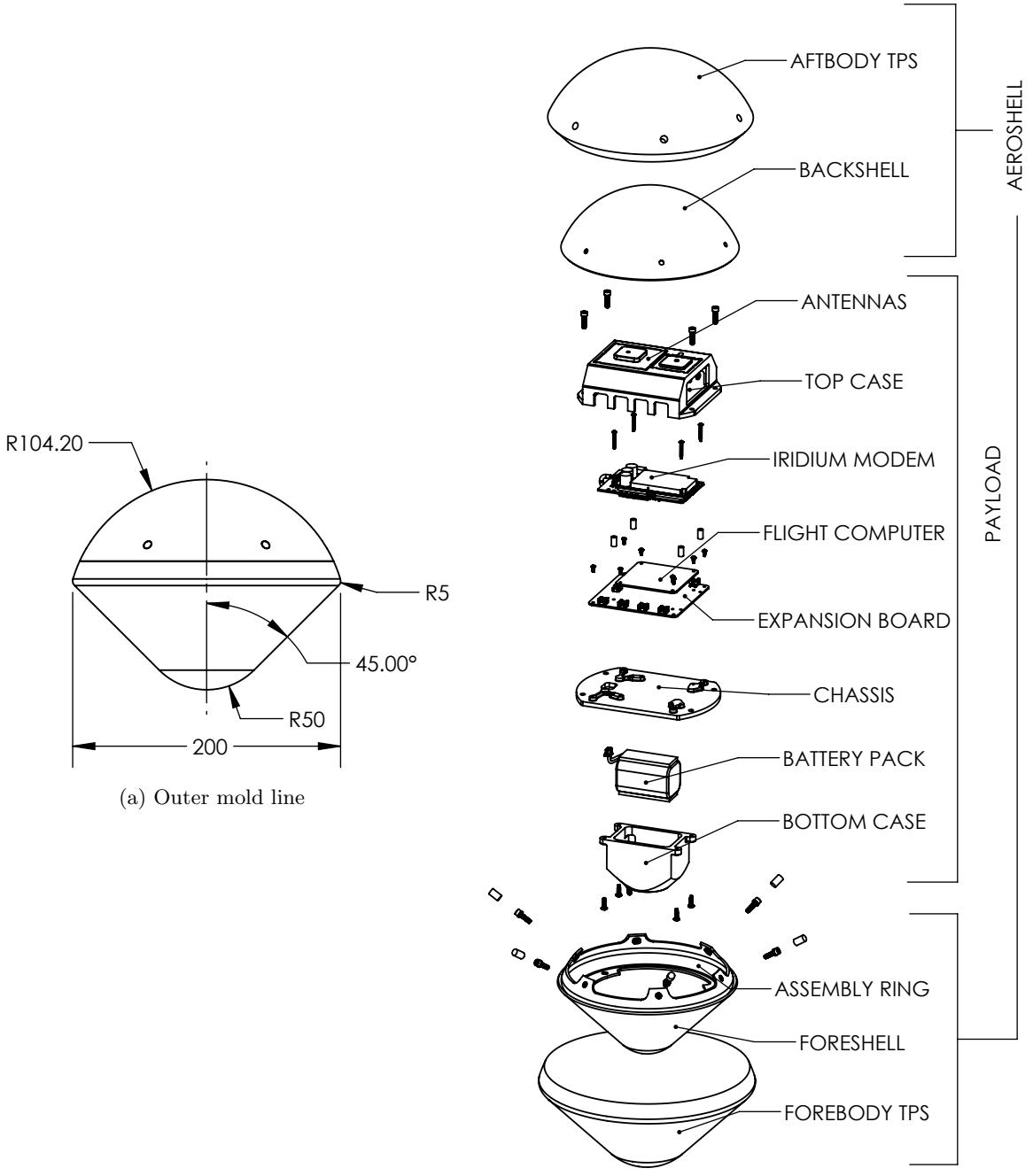

(a) Outer mold line

(b) Exploded view

Figure 6: RED-Data2 vehicle overview.

Table 6: RED-Data2 mass breakdown.

Component	Material	CBE Mass (kg)	Contingency (%)	CBE + Contingency Mass (kg)	
Forebody TPS	C-PICA	0.175	0*	0.175	
Aftbody TPS	C-SICA	0.151	0*	0.151	
Foreshell	Carbon Fiber	0.119	20	0.143	
Backshell	Carbon Fiber	0.121	20	0.145	
Assembly Ring	Carbon Fiber	0.076	20	0.091	
Bottom Case	POM	0.083	10	0.091	
Top Case	POM	0.074	10	0.081	
Chassis	POM	0.065	10	0.072	
Battery Pack	multiple	0.071	20	0.085	
AFC	multiple	0.02	10	0.022	
EBM	multiple	0.025	50	0.038	
Iridium Modem	multiple	0.075	20	0.090	
GPS Antenna Module	multiple	0.006	0	0.006	
Iridium Antenna Module	multiple	0.015	10	0.017	
Mechanical Hardware	multiple	0.025	25	0.031	
Electrical Interconnects	multiple	0.05	25	0.063	
				1.300	Total
				1.430	Total+10% Margin

are available from Mars Microprobe analyses.[9,10] Additional aerodynamic data for the subsonic regime including pitch moments are available from wind tunnel testing on a REBR scale model performed at NASA Ames Fluid Mechanics Laboratory.[16] These results drive center of gravity (CG) placement in the REBR design,[1] constraints which are adopted here.

To ensure static stability and trim limits of 3.5° in hypersonic flight, 10° in transonic flight and 7° in subsonic flight, the CG is placed within an envelope of $\pm 0.01D$ in the lateral direction measured from the centerline and $0.30 - 0.44D$ in the longitudinal direction measured from the nose. Nominally, the RED-Data2 CG is located a distance 0.41D from the nose and 0.01D from the centerline. Proper longitudinal CG placement is achieved by locating the payload as far forward toward the nose as possible given volume constraints. No ballast is required to move the CG within the design envelope.

VII.B.2. Trajectory

The nominal ISS return and orbital decay entries are shown in Figure 7. Breakup, modeled for altitudes of 65km, 75km and 85km, produces a step change in velocity due to the instantaneous change in ballistic coefficient (Figure 7a). Breakup points are indicated by circles. The trajectory is largely independent of entry conditions and breakup altitude below about 35km. Correspondingly, transmit time, with transmission starting around 25km, is equivalent across the trajectories. Figure 7c shows this common portion of the trajectory below 35km before and after the start of transmission.

The start of data transmission is further illustrated by the zenith angle criterion shown in Figure 7d. Here, zenith angle is plotted from breakup until ground impact for the ISS return with 85km breakup altitude. The time scale has been shifted so $\phi = 10°$ occurs at 0 sec. At breakup (upper left), the flight path angle has not changed significantly from the entry angle and RED-Data2 is flying nearly horizontally. Therefore, zenith angle is close to 90° (that is, the Iridium antenna is pointing toward the horizon). About two minutes after breakup, flight path angle rapidly decreases (as does zenith angle) as the vehicle undergoes a gravity turn. Zenith angle finally falls below 10° with 418 sec (6.97 min) of available transmit time until ground impact. About 50 sec into transmission, flight path angle approaches −90°, and the Iridium antenna points directly toward the zenith ($\phi = 0°$).

Trajectories are plotted over time in Figure 7b. From atmospheric interface, reentry lasts 913 sec (15.2 min) for the ISS return and 1363 sec (22.7 min) for the orbital decay entry (with some variation due to breakup altitude). During entry, RED-Data2 is attached to the host between 226–351 sec (3.8 – 5.9 min) and 658 – 804 sec (11.0 – 13.4 min) for the ISS return and orbital decay entries, respectively. On the REBR flights, reentry was detected at approximately 90km. For RED-Data2, the host passes this altitude 196 sec and 611 sec after entry interface, respectively, for ISS return and orbital decay. Assuming comparable reentry detection, RED-Data2 will record data on the host for 30–155 sec (ISS return) and 47–193 sec (orbital decay). If RED-Data2 records data for an additional minute after breakup, as on REBR, then total record time ranges from 90–215 sec (ISS return) and 107–253 sec (orbital decay). It is reasonable to expect record time to be at the upper end of these ranges. REBR experienced breakup at the lower end of the altitude range (66.5km on HTV2),[1] and 78km is considered a typical breakup altitude for unprotected spacecraft.[5] More sensitive reentry detection can increase the recording time, which would be important for those missions expected to breakup higher in the atmosphere. A lower ballistic coefficient host (such as HTV) also extends available recording time.

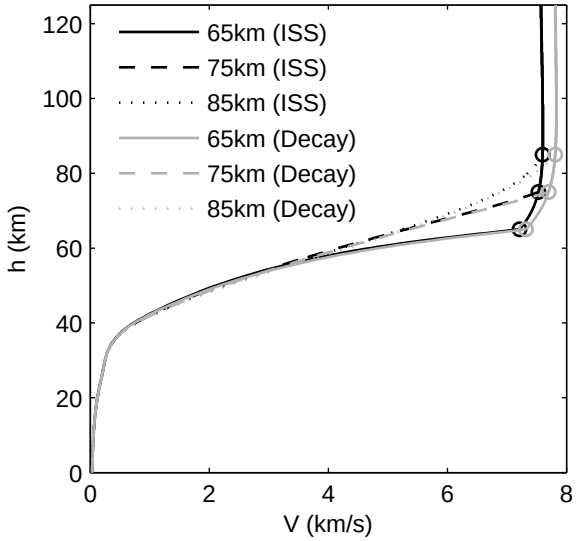

(a) Altitude vs. velocity

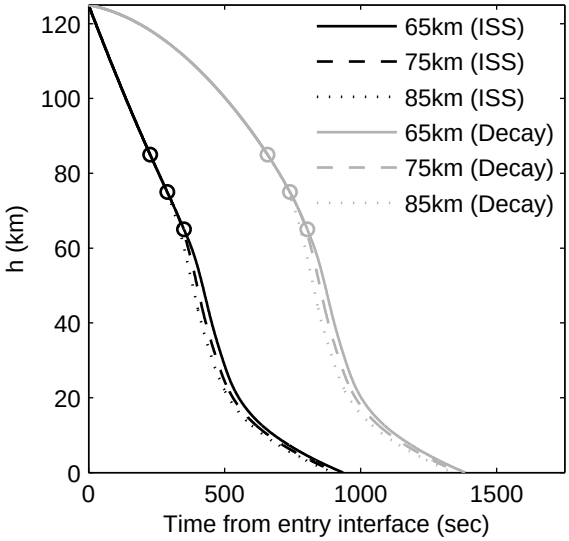

(b) Altitude vs. time

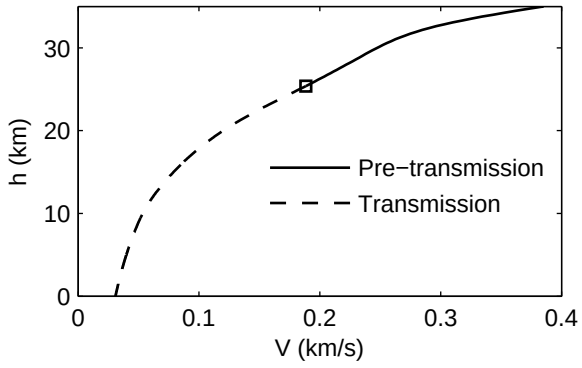

(c) Altitude vs. velocity (below 35km)

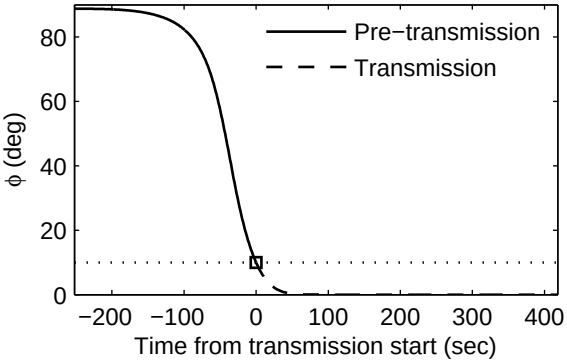

(d) Zenith angle from transmission start (ISS return, 85km breakup altitude)

Figure 7: Nominal entry trajectories for RED-Data2.

VII.B.3. Electronics

The electronics package consists of a pair of modular PCBs (printed circuit boards): the Avionics Flight Computer (AFC) and Expansion Board Module (EBM) shown in block diagram format in Figure 8. Core functionalities such as recording and storing flight data and commanding external hardware are provided by the AFC while the EBM provides specialized functionality. The modular design allows a common AFC to be paired with a unique EBM designed to meet host- or mission-specific requirements. For example, the baseline EBM in Figure 8 includes circuitry to interface with the external thermocouples in an instrumented TPS. Support for other hardware components such as the Iridium modem is also accomplished through the EBM.

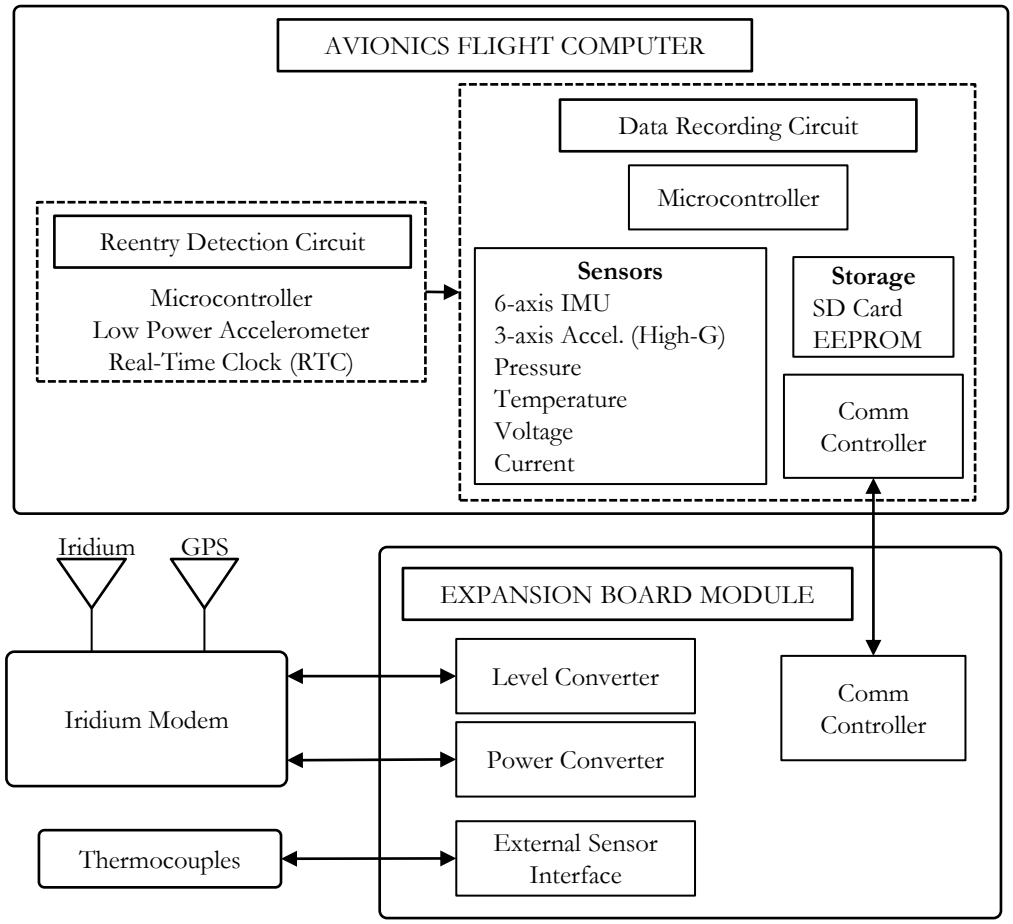

Figure 8: Block diagram of RED-Data2 electronics.

The AFC is further divided into a reentry detection circuit and a data recording circuit. The data recording circuit includes a suite of COTS (commercial off-the-shelf) sensors listed in Table 7. These include a MEMS 6-axis inertial measurement unit (IMU), 3 high-g single-axis accelerometers, and a barometer, in addition to onboard voltage, current and temperature sensors to monitor hardware health. The single-axis accelerometers are mounted in each of the X, Y and Z body axes (where the X-axis is aligned with the centerline of the vehicle and is positive toward the nose). The X-axis accelerometer is contained on a small daughter PCB mounted perpendicularly to the main AFC board. The reentry detection circuit is minimally constructed with a low power COTS accelerometer (Bosch BMA250), microcontroller and real-time clock (RTC) for alarm scheduling and timestamps. The BMA250 contains built in interrupt logic that can detect certain acceleration-based events. These interrupts in turn activate the microcontroller (from sleep mode) to perform more complex calculations from the BMA250 output and determine whether reentry has begun. Reentry detection is discussed later in detail.

Table 7: Avionics Flight Computer (AFC) Sensors.

Manufacturer	Part Number	Description	Range	Qty
Invensense	MPU-6000	6-Axis IMU	±16g, ±2000°/sec	1
Analog Devices	ADXL193	1-Axis Accelerometer	±250g	3
Freescale Semiconductor	MPXH6115A6T1	Barometer	30–110 kPa (4.35–15.95 psi)	1
Texas Instruments	TMP275	Temperature Sensor	20–100°C (-4–212°F)	1
Texas Instruments	INA139	Current Sensor	Full Operational Range	1
(onboard voltage divider)	–	Voltage Sensor	Full Operational Range	1

The baseline EBM includes drivers and connectors to support up to 8 thermocouples. Four 2-pin, 2mm pitch thermocouple connectors are mounted along each of the two long edges of the EBM board. A 9-pin Molex Pico-Clasp^{TM} wire-to-board connector connects the EBM to the Iridium modem. The 60mm square AFC lies flush against the larger, 88mm x 84mm, EBM, and the two are electrically connected via header pins soldered into each board. Prototype versions of the AFC and EBM are shown in Figure 9. The AFC shown is a development unit with several components added or replaced from the final hardware. Board dimensions, however, are accurate. The EBM is a prototype only and is not representative of final hardware components nor size.

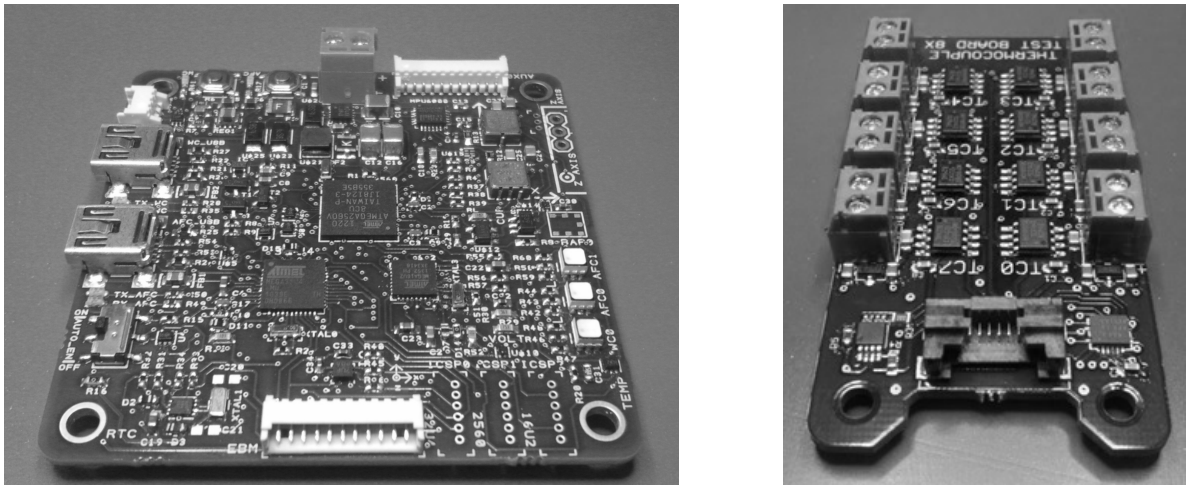

Figure 9: Avionics flight computer (AFC) (left) and representative expansion board module (EBM) (right).

VII.B.4. Communications

The A3LA-RG Iridium Modem (from NAL Research Corporation) provides Iridium communication and GPS reception for RED-Data2. To conserve space internally, the modem hardware is removed from its standard 4.0 x 2.43 x 0.95 in. enclosure, reducing the overall package to a 3.33 x 2.09 x 0.74 in. rectangular envelope. The A3LA-RG includes a female 25-pin connector (DB-25) for connection to an Iridium handset. Only 9 of these pins are required for RED-Data2. The DB-25 connector is removed and replaced with a soldered wire harness terminated by 9-pin wire-to-board connector which is the mated pair to the 9-pin EBM connector.

The maximum data rate over the Iridium network is 2400 bps (bits per second). In practice, actual data rate is somewhat less.[1] Conservatively, if half the maximum rate is achieved (1200 bps), RED-Data2 can return about 61kB of data in the available transmit time (418 sec). With a maximum recording time of 253 sec, the data recording rate averages at least 248 bytes / sec for the orbital decay entry. Similarly, recording rate averages at least 292 bytes / sec over a maximum recording time of 215 sec in the ISS return.

Iridium communications are carried on L band frequencies in the 1616MHz – 1626.5 MHz range. RED-Data2 utilizes a 25mm x 25mm x 4mm Iridium patch antenna manufactured by Taoglas for this purpose. The antenna is mounted to a 50mm square PCB ground plan with a surface-mounted microcoaxial connector

for wiring to the modem. A coaxial cable connects the antenna module to the modem board.

Close proximity of the GPS L1 frequency (1575.42MHz) to the Iridium band necessitates RF interference mitigation. A COTS GPS module was selected with front-end SAW (surface acoustic wave) filter to reject out band frequencies in the Iridium range. The module consists of a 25mm x 25mm x 2mm ceramic patch antenna mounted to a 35mm square ground plane. A coaxial cable with microcoaxial connector comes pre-soldered to the PCB. Its free end connects to a corresponding connector on the modem board.

VII.B.5. Power

RED-Data2 is powered by four Energizer L91 Ultimate Lithium AA batteries in a 2x2 pack configuration. The batteries employ a lithium-iron disulfide chemistry providing 1.5V nominally and approximately 3 Amp-hrs capacity. The batteries largely maintain capacity across a wide temperature range (-40°C – 60°C). On REBR, the cells were qualified up to 76°C.[1] The large reduction in number of batteries over the REBR design (from 24 AAs to 4 AAs) is enabled by low power electronics, particularly the reentry detection circuit which operates at around 0.9mW while awaiting reentry.

The four AAs are connected in series to form a 6V, 3 Amp-hr pack. Soldered wires connect adjacent battery terminals. A plastic (Delrin) frame locates and structurally supports the cells. The entire pack is wrapped in tape and shrinkwrapped in plastic for mechanical constraint. A 2-wire harness exits the side of the pack and terminates with a 2-pin connector, which plugs into the bottom side of the EBM. A Molex Duraclik^{TM} 2mm pitch, wire-to-board connector was selected for its locking mechanism and performance in high vibration environments.

During sleep and reentry detection, the electronics draw approximately 0.15 mA. When reentry is detected, the AFC enters data recording mode and remains powered on for the remainder of the flight, drawing drawing 0.1 A for a maximum of 12.5 min in the orbital decay trajectory (0.021 Amp-hrs). After data recording, RED-Data2 will initiate a call and transmit data through its Iridium modem until surface impact. The modem draws about 0.5 A over the transmit time of 418 sec (0.06 Amp-hrs). In total, the reentry will use a 0.08 Amp-hrs for data recording and transmission leaving 2.92 Amp-hrs for Pre-Launch, Launch and Reentry Detection phases, or about 2.2 years of operations (unmargined).

VII.B.6. Structure

A chassis and top and bottom cases comprise the payload structure (Figure 10). All three components are machined from polyoxymethylene (POM), a thermoplastic polymer with good strength, hardness and rigidity under temperature extremes that was utilized on REBR. The 4mm thick chassis provides the primary load-bearing structure to which the electronics and cases attach. The EBM, AFC and modem mount via screws to the top of the chassis forming the PCB stackup. The modem is offset above the other boards by cylindrical standoffs.

The top case rests on top of the chassis over the PCB stackup. The GPS and Iridium antennas are affixed to the top of this case, oriented to radiate out the backshell. The battery pack inserts into the bottom case, which provides mechanical support and thermal insulation. Urethane foam pieces above and below constrain the pack and provide vibration damping. This case attaches to the bottom surface of the chassis via screws. All screw attachments are made with trilobular thread forming screws, which allow for easy assembly and disassembly. The chassis, cases and electronics form the payload assembly. The payload assembly bolts at four locations to an assembly ring that is fixed to the interior wall of the foreshell.

Structural components were designed to minimize complexity and cost. The chassis and cases can be easily machined on a CNC mill, and a low part count is maintained. Future designs could leverage 3D printing with an alternate plastic for simple, low cost fabrication.

Worst-case deceleration loads of 10g and 10.4g, for the ISS return and orbital decay entry, respectively, are expected after breakup (Figure 11). Following the REBR specification, structural components are designed to withstand loads that far exceed the nominal, up to 100g in the axial direction and ±9g in off-axial directions, due to large uncertainties in the breakup environment.

VII.B.7. Thermal Protection System

RED-Data2 utilizes a conformal ablative thermal protection system (TPS) developed by NASA Ames Research Center.[17] Conformal TPS has the potential to simplify manufacturing and assembly and reduce cost

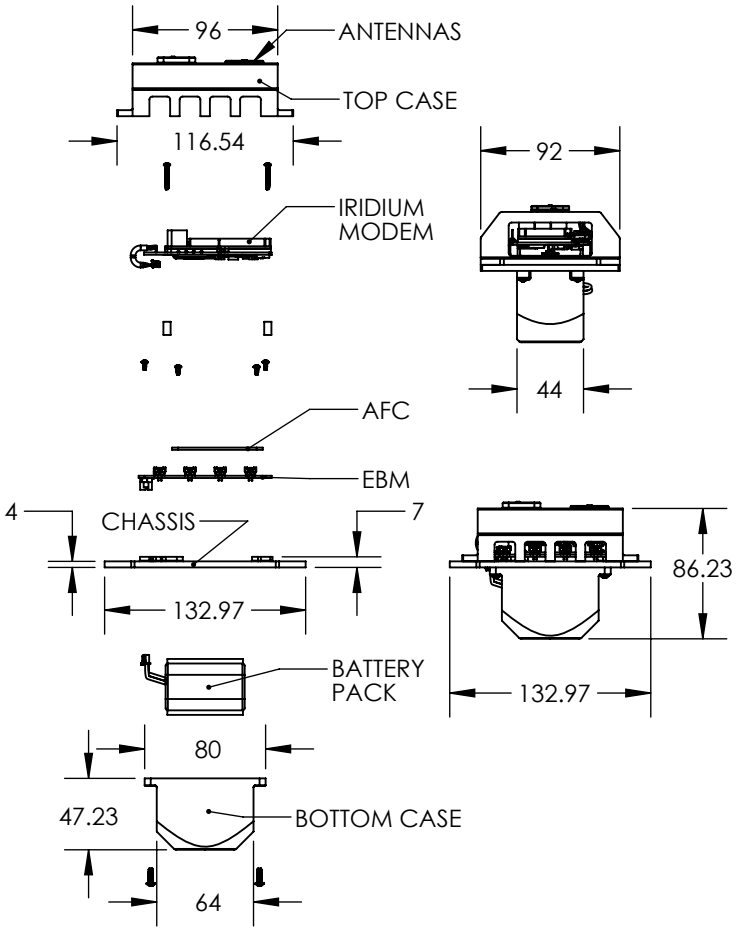

Figure 10: Major dimensions of payload assembly (in millimeters).

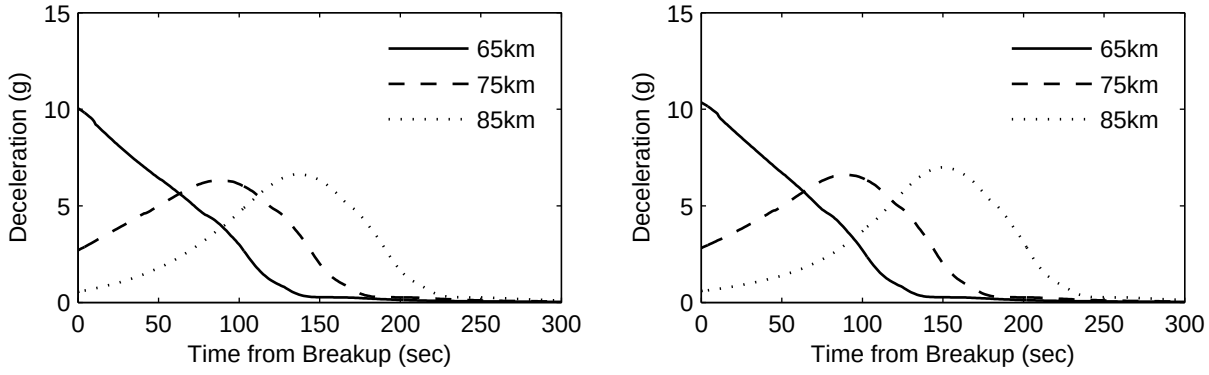

(a) ISS return

(b) Orbital decay entry

Figure 11: Deceleration loads for nominal trajectories.

by utilizing flexible, high strain-to-failure component materials that can be formed in large segments and directly bonded to an aeroshell without gap filler.

A carbon-based variant of this material (C-PICA) which can withstand heating up to at least 500 W/cm^2 forms the forebody TPS. The aftbody TPS is a silica-based variant (C-SICA) that is RF-transparent to allow Iridium and GPS transmission through the backshell.

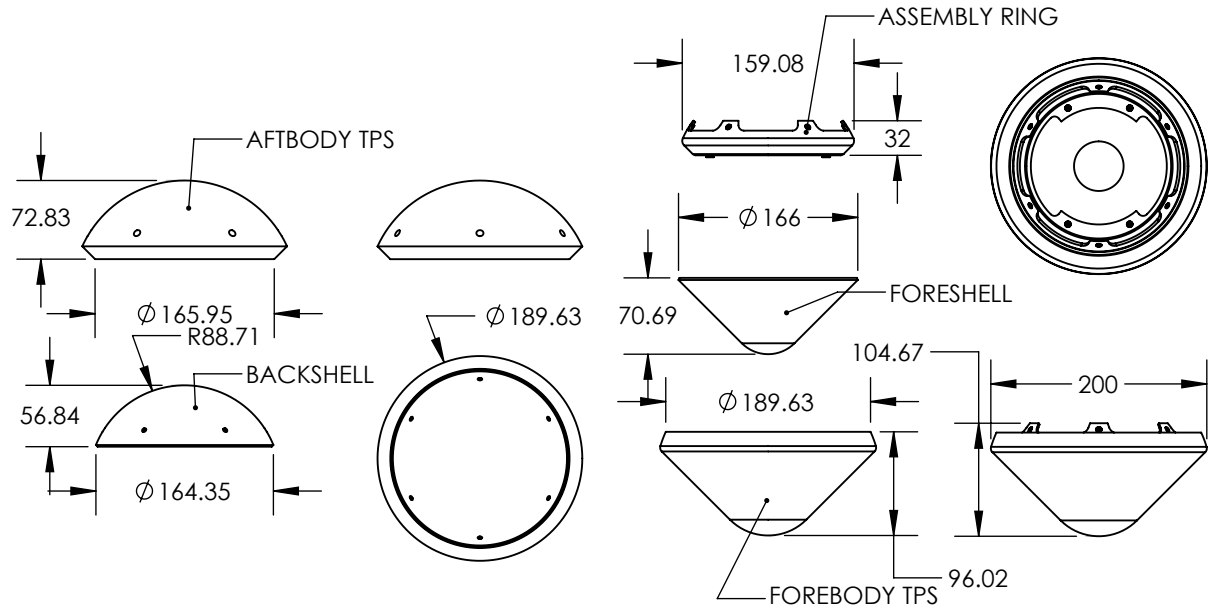

(a) Major dimensions of aft aeroshell (in millimeters).

(b) Major dimensions of forward aeroshell (in millimeters).

Figure 12: RED-Data2 aeroshell configuration.

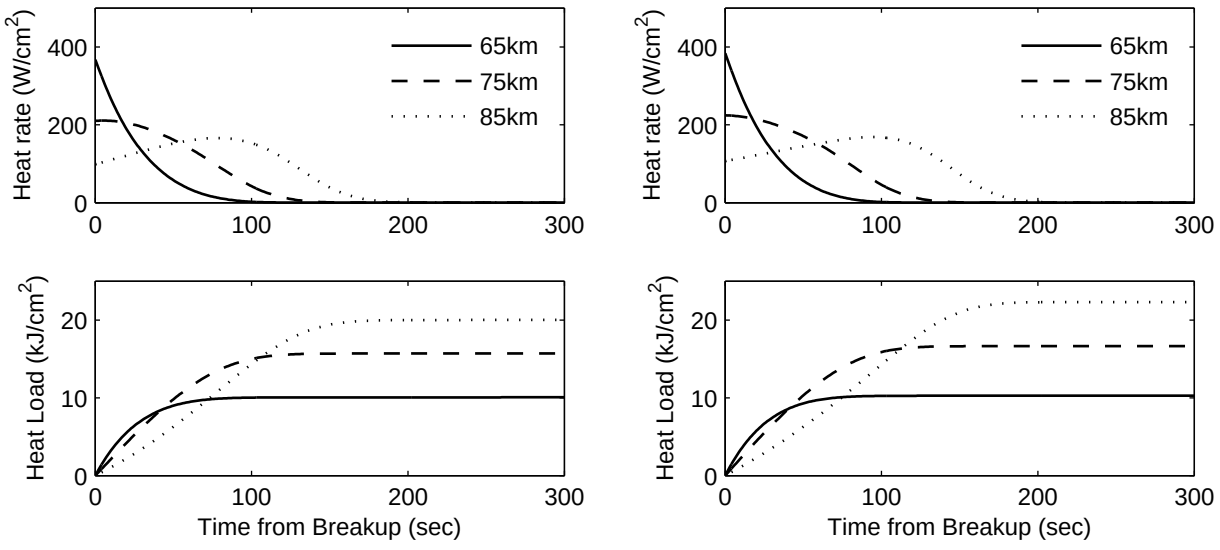

(a) ISS return

(b) Orbital decay entry

Figure 13: Stagnation heat rate and integrated heat load for nominal trajectories.

The TPS segments are adhered to composite shells which form the aeroshell structure (Figures 12a and

12b). Installed inside the foreshell is the composite assembly ring. Tabs on the ring extend up into the backshell to bolt the two halves of the aeroshell together at six locations.

The TPS is uniformly 1.55cm thick around the entire body to protect against potential aftbody heating while still attached to the host. Peak heat rate and integrated heat loads at the stagnation point were evaluated for the nominal trajectories (Figure 13). The highest peak heat rate occurs at the lowest breakup altitude (65km) and is a maximum at the point of breakup. For lower breakup altitudes, heat rate peaks some time after breakup. Maximum heat rate is 368 W/cm^2 for the ISS trajectory and 384 W/cm^2 for the orbital decay trajectory, which is well within the capability of C-PICA. The maximum heat load occurs at the highest breakup altitude (85km), where the capsule experiences the longest exposure to aeroheating, 20.0 kJ/cm^2 and 22.3 kJ/cm^2 for the ISS and orbital decay cases, respectively. The TPS was sized to the maximum heat load case and a bondline temperature limit of 250°C.

VII.C. Flight Software

RED-Data2 flight software is currently under design with the aim to expand its applicability to arbitrary entries from LEO. RED-Data2 software initially puts the hardware into sleep mode during launch. The RTC then wakes the reentry detection circuit at a pre-specified time when the host is on-orbit. Then, the software enters into a continuous reentry detection mode.

The reentry detection algorithm must distinguish between reentry and non-reentry events, such as on-orbit maneuvering or uncontrolled tumbling. The BMA250 and microcontroller pair contained in the reentry detection circuit perform this function. The built-in logic of the BMA250 allows it to trigger an interrupt when the acceleration measured in any of its three axes (X, Y, Z) surpasses a specified threshold. At the finest resolution, this threshold can assume values that are multiples of 7.81 mg (milli-g, 1/1000 of gravitational acceleration) up to 2g. The threshold can be set dynamically on-orbit by waking the microcontroller up at specified intervals via the RTC. This capability can be used to adjust for changes in the on-orbit state of the host.

The interrupt signal generated by the accelerometer then activates the microcontroller, which can perform more complex calculations such as a root-mean-squared (RMS) calculation over all axes to estimate total acceleration on the vehicle. The acceleration profile over time is used to distinguish between reentry and non-reentry events. For example, a deorbit burn would produce a relatively short, constant acceleration. Reentry, however, produces a small, but increasing, acceleration due to atmospheric drag.

Dynamic sampling allows high sampling rates while attached to the host to facilitate trajectory reconstruction and breakup modeling. REBR collected IMU data at 4 Hz, not enough for high fidelity attitude reconstruction during the dynamic breakup environment. The IMU data was numerically upscaled in subsequent reconstruction efforts to 80 Hz.[18] On RED-Data2, sampling rate is still limited by total data return. However, a lower sampling rate after breakup is traded for higher rate beforehand to capture breakup dynamics. Representative sampling rates for the nominal entries are shown in Table 8. The data rates indicated provide at least 10% margin in the total data budget of 61kB, assuming that sampling rates are lowered to match those of REBR after breakup. Data rates are computed for the maximum recording time, i.e. lowest breakup altitude. When data collection ends, a connection with Iridium is attempted. Once connection is

			ISS Return		Orbital Decay	
Sensor	Qty	Sample Size (bits)	Sampling Rate (Hz)	Data Rate (bytes / sec)	Sampling Rate (Hz)	Data Rate (bytes / sec)
IMU	1	48	30	180	25	150
High-G Accel	3	8	30	90	25	75
Thermocouple	8	8	8	8	1	8
Pressure	1	8	0.5	0.5	0.5	0.5
Current	1	8	0.5	0.5	0.5	0.5
Voltage	1	8	0.5	0.5	0.5	0.5
		Total		279.5		234.5

Table 8: Sampling rates for nominal entries.

established, the recorded data is transmitted until ground impact destroys the vehicle.

VII.D. Ground System

Data recovery is accomplished via transmission over the Iridium Router-Based Unrestricted Digital Internetworking Connectivity Solutions (RUDICS) system. RUDICS provides two-way data service for Iridium devices over a TCP/IP connection. An Iridium call placed by the onboard modem is seamlessly routed over the Internet through the ground-based RUDICS gateway to a server residing in the Space Systems Design Laboratory at Georgia Tech. The ground server runs a simple Python script that continuously listens for this TCP/IP connection on a pre-specified port and IP address. When connection is established, any incoming data is then logged to a file. Data is transmitted in binary format and can be encrypted to mitigate risk in case of interception.

This communication system, successfully demonstrated on REBR,[1] significantly reduces mission complexity. It eliminates the need for physical recovery of the capsule. Therefore, neither a parachute or other recovery device, which add mass, cost and risk, is needed nor are ground operations to retrieve the device. It also reduces ground infrastructure requirements by offloading the complication of space-to-ground communication to an intermediary (RUDICS). The only physical system required is a basic server and Internet connection.

VIII. Conclusion

Getting into orbit is increasingly possible with CubeSats and other small satellites. Analogous systems that can return to Earth, however, are limited. Small reentry probes address this gap in capability, providing the potential for reentry data recording, flight testing and payload return. To reduce uncertainty and improve our ability to predict surviving debris, impact time and impact location, reentry breakup dynamics and aerothermodynamics data is needed. REBR demonstrated the promise of a device that can provide such information. The challenge now is to bring this technology to a broader market by making it smaller, lighter and more usable across a range of missions and host vehicles.

RED-Data2 is the first step toward realizing this goal. It offers several advantages over REBR which can make adoption by satellite and launch vehicle providers more widespread. RED-Data2 is closer to the size of a softball as opposed to a basketball. It is also more than 50% lighter, autonomously initiated, and capable of passive in-space operations for a year or more as opposed to months. In addition, the flexibility of the RED-Data2 design, manifested in the structural design and modular electronics approach, allows expansion of functionality to future RED vehicles.

Parts of the design have already been fabricated, and future work aims to produce the first complete flight unit. The electronics are under active development with the goal to produce a redundant, fault-tolerant design. Software efforts are focused on autonomous activation of RED upon reentry as well as an intelligently adjusted sensor sampling rate according to user-specified priority (e.g. high frequency sampling during breakup). Work is underway to assess fabrication of the aeroshell and payload structure.

Acknowledgments

The authors would like to acknowledge Mr. Dominic DePasquale of Terminal Velocity Aerospace, for guidance and direction on the RED-Data2 design, and Mr. Michael Cato of BitFox Electronics, for invaluable assistance designing, fabricating and programming electronics hardware. In addition, Mr. Jeremy Hill, Mr. Amit Mandalia, Dr. Milad Mahzari, and Dr. Soumyo Dutta contributed to the initial concept study. Dr. Dutta receives special thanks for help with developing trajectory codes. Finally, the authors are grateful to the Georgia Research Alliance for their financial support of this work.

References

[1]Weaver, M. and Ailor, W., "Reentry Breakup Recorder: Concept, Testing, Moving Forward," *AIAA Space Conference*, September 2012, AIAA 2012-5271.

[2]Ailor, W., Dupzyk, I., Shepard, J., and Newfield, M., "REBR: An Innovative, Cost-Effective System for Return of Reentry Data," *AIAA Space Conference*, September 2007, AIAA 2007-6222.

[3]Kapoor, V. B. and Ailor, W. H., "The Reentry Breakup Recorder: A Black Box For Space Hardware," *17th Annual AIAA/USC Conference on Small Satellites*, 2003.

[4]Buchen, E. and DePasquale, D., "2014 Nano / Microsatellite Market Assessment," January 2014.

[5]Ailor, W. H., Rasky, J. D., and Zell, P., "Pico Reentry Probes: New Tools for Reentry Testing," *56th International Astronautical Congress*, October 2005.

[6]Ailor, W. H., Carroll, J. A., Rasky, J. D., and Ridenoure, R., "Pico Reentry Probes: Partnership Pushes Evolution," *AIAA Space Conference*, September 2006, AIAA 2006-7528.

[7]Sidor, A., Braun, R., and DePasquale, D., "RED-Data2 Commercial Reentry Recorder: Size Reduction and Improved Electronics Design," *AIAA SciTech Conference*, January 13-17 2014, AIAA 2014-1231.

[8]Smrekar, S., e. a., "Deep Space 2: the Mars Microprobe Mission," *Journal of Geophysical Research: Planets*, Vol. 104, 1999, pp. 27013–27030.

[9]Mitcheltree, R., Moss, J., Cheatwood, F., Greene, F., and Braun, R., "Aerodynamics of the Mars Microprobe Entry Vehicles," *Journal Of Spacecraft And Rockets*, Vol. 36, No. 3, May-June 1999, pp. 392–398.

[10]Braun, R., Mitcheltree, R., and Cheatwood, F., "Mars Microprobe Entry-to-Impact Analysis," *Journal Of Spacecraft And Rockets*, Vol. 36, No. 3, May-June 1999, pp. 412–420.

[11]Willcockson, W. H., "Stardust Sample Return Capsule Design Experience," *Journal Of Spacecraft And Rockets*, Vol. 36, No. 3, May-June 1999, pp. 470–474.

[12]Desai, P., Mitcheltree, R., and Cheatwood, F., "Entry Dispersion Analysis for the Stardust Comet Sample Return Capsule," *Journal Of Spacecraft And Rockets*, Vol. 36, No. 3, May-June 1999.

[13]Grinstead, J. H., P., J., Cassell, A. M., Alberts, J., and Winter, M. W., "Airborne Observation of the Hayabusa Sample Return Capsule Re-entry," *42nd AIAA Thermophysics Conference*, Honolulu, June 2011, AIAA 2011-3329.

[14]Vinh, N., Busemann, A., and Culp, R., *Hypersonic and Planetary Entry Flight Mechanics*, The University of Michigan Press, 1980.

[15]Sutton, K. and Graves, R. A., "A General Stagnation-Point Convective-Heating Equation for Arbitrary Gas Mixtures," *NASA TR-R-376*, November 1971.

[16]Jones, L., Rudo, A., Stavros, K., Welsh, R., Wittenberg, R., and Zanacic, A., "Force and Moment Measurements on a 2/3 Scale Model of Re-Entry Breakup Recorder (REBR)," NASA Ames Fluid Mechanics Laboratory.

[17]Beck, R., Arnold, J., Gasch, M., Stackpoole, M., Prabhu, D., Szalai, C., Wercinski, P., and Venkatapathy, E., "Conformal Ablative Thermal Protection System for Planetary and Human Exploration Missions: An Overview of the Technology Maturation Effort," *10th Annual Interplanetary Probe Workshop*, July 2013.

[18]Patera, R., "Attitude Reconstruction Analysis Of The Reentry Breakup Recorder," *23rd AAS/AIAA Space Flight Mechanics Meeting*, February 2013.